Physics of Fluids

Symmetric and asymmetric coalescence of droplets on a solid surface in the inertia-dominated regime

Cite as: Phys. Fluids **31**, 092106 (2019); https://doi.org/10.1063/1.5119014
Submitted: 08 July 2019 . Accepted: 04 September 2019 . Published Online: 20 September 2019

Nilesh D. Pawar, Supreet Singh Bahga, Sunil R. Kale, and Sasidhar Kondaraju

Physics of Fluids ARTICLE scitation.org/journal/phf

Symmetric and asymmetric coalescence of droplets on a solid surface in the inertia-dominated regime

Cite as: Phys. Fluids 31, 092106 (2019); doi: 10.1063/1.5119014
Submitted: 8 July 2019 • Accepted: 4 September 2019 •
Published Online: 20 September 2019

Nilesh D. Pawar,[1,2] Supreet Singh Bahga,[2] Sunil R. Kale,[2] and Sasidhar Kondaraju[3,a)]

AFFILIATIONS

[1]Department of Mechanical Engineering, Walchand College of Engineering Sangli, Sangli, Maharashtra 416415, India
[2]Department of Mechanical Engineering, Indian Institute of Technology Delhi, Hauz Khas, New Delhi 110016, India
[3]School of Mechanical Sciences, Indian Institute of Technology Bhubaneswar, Argul, Odisha 752050, India

[a)]**Electronic mail:** sasidhar@iitbbs.ac.in

ABSTRACT

We present an investigation of symmetric and asymmetric coalescence of two droplets of equal and unequal size on a solid surface in the inertia-dominated regime. Asymmetric coalescence can result due to the coalescence of two unequal-sized droplets or coalescence of two droplets having different contact angles with the surface due to a step gradient in wettability. Based on the solution of an analytical model and lattice Boltzmann simulations, we analyze symmetric and asymmetric coalescence of two droplets on a solid surface. The analysis of coalescence of identical droplets show that the liquid bridge height grows with time as $(t^*)^{1/2}$ for $\theta = 90°$ and $(t^*)^{2/3}$ for $\theta < 90°$, where t^* is dimensionless time. Our analysis also yields the same scaling law for the coalescence of two unequal-sized droplets on a surface with homogeneous wettability. We also discuss the coalescence of two droplets having different contact angles with the surface due to a step gradient in wettability. We show that the prediction of bridge height with time scales as $(t^*)^{2/3}$ irrespective of contact angles of droplet with the surface.

I. INTRODUCTION

When two liquid droplets come in contact, they merge to form a single droplet. This process is known as coalescence of droplets. During the early stage of the coalescence process, two liquid droplets are connected by a liquid bridge of infinite curvature at the point of contact as shown in Fig. 1. The large curvature induces significant Laplace pressure which drives the liquid into the bridge[1–3] and, consequently, the height of a liquid bridge h_0 grows with time t. The dynamics of droplet coalescence depends on whether the coalescence droplets are freely suspended or placed on a substrate. Coalescence of freely suspended droplets is important in coalescence of rain drops[4] and cloud formation.[5] However, there are practical applications where droplets placed on a substrate coalesce with others. This form of coalescence is usually observed during dropwise condensation,[6,7] inkjet printing,[8] and spray coating.[9]

Coalescence of freely suspended droplets has been extensively studied.[9–14] Eggers *et al.*[15] studied the Strokes regime of coalescence both analytically and numerically. Their results revealed that the bridge radius grows with time as $t \log t$. Later, Duchemin *et al.*[9] were the first to find that the bridge height grows with time as $t^{1/2}$ in the inertial regime. However, the coalescence of droplets on a solid substrate differs from the coalescence of freely suspended droplets. This is because the presence of a solid surface slows down the transport of liquid toward the bridge. However, the most interesting observations can be made in the early stage of coalescence. The meniscus profile $y(x, t)$ during the early stage of coalescence is governed by a single length scale and follows the self-similar dynamics.[16,17] The dynamics of the bridge profile are studied in terms of the growth of the liquid bridge height with time. Ristenpart *et al.*[18] conducted an experimental and theoretical investigation to study the coalescence of two spreading droplets on a highly wettable surface. They observed that the width of the meniscus bridge d_m grows with time t as

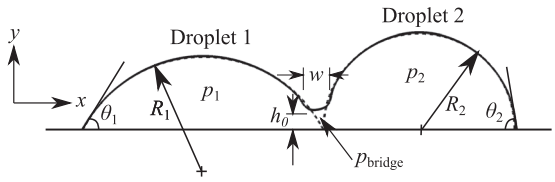

FIG. 1. Schematic illustrating the coalescence of two droplets of same liquid having different contact angles with the surface due to a step gradient in surface wettability. The dotted line shows the initial droplet profile and the solid line shows the droplet profile after bridge formation. Here, p, R, and θ are the pressure, radius, and contact angle of the surface, respectively, whereas, subscripts 1 and 2 represents the properties of droplet 1 and 2, respectively. Furthermore, h_0, w, and p_{bridge} denotes the liquid bridge height, radius of curvature of bridge, and pressure in the bridge.

$d_m \sim (h_0^{3/2}/R_0)(\sigma t/\mu)^{1/2}$, where R_0, h_0, σ, and μ denote the radius, height, surface tension, and viscosity, respectively. However, the analysis of Ristenpart *et al.* was restricted to a surface with contact angle close to zero. Later, Narhe *et al.*[19] reported coalescence of two droplets on a partial wetting surface and showed that bridge height grows linearly with time. In their experiments, coalescence of droplets was instigated either by condensation or by the syringe deposition. In a related publication, Lee *et al.*[20] performed experiments on a partial wetting surface with a contact angle of $10^\circ \le \theta \le 56^\circ$. They demonstrated that bridge height R_y follows the scaling law $R_y/R_0 = (3\sigma t/4\ \mu R_0 \tan\theta)^\alpha$, where the power law exponent α varies in the range of $0.51 \le \alpha \le 0.86$. Hernández-Sánchez *et al.*[16] investigated coalescence of different contact angle droplets leading to asymmetric coalescence. They showed that the bridge height grows linearly with time. Furthermore, the initial growth shows self-similar behavior. Recently, Thete[21] studied the singularity which arises during the coalescence of droplets using a combination of theory, experiments, and numerical simulations.

The majority of previous studies on droplet coalescence, including those mentioned above were performed in the regime where viscous effects dominate inertia. However, the viscous forces are negligible when the characteristic length scale, i.e., bridge height h_0 is much greater than the viscous length scale $h_0 \gg l_v$, where $l_v = \mu^2/(\sigma\rho)$, where μ, ρ, and σ denote the viscosity, density, and surface tension of liquid, respectively.[9,13] For low viscosity liquids, such as water, viscous length l_v is of $\mathcal{O}(10\,\text{nm})$ and, therefore, the coalescence process always occurs in the regime where inertia dominates viscous effects. Therefore, it is essential to understand the coalescence of droplets in the inertia-dominated regime. Recently, Paulsen *et al.*[22,23] proposed a new inertially limited viscous regime, where surface tension, viscous, and inertia forces all balance for all viscosity fluids.

The inertial coalescence of droplets on a solid substrate was first reported by Eddi *et al.*[24] They observed that the growth of bridge for droplets coalescing on a partial wetting substrate differs depending on whether the substrate is of neutral wetting ($\theta = 90^\circ$) or hydrophilic ($\theta < 90^\circ$). The bridge height is found to grow similar to freely suspended droplets on a neutral wetting substrate, and it grows with time as $t^{2/3}$ on a hydrophilic substrate. Later, Sui *et al.*[25] showed that the exponent of power law, for an increase in bridge height with time, depends on time. The exponent is 2/3 up to a certain critical time and beyond which it transitions to 1/2. For a surface with $\theta = 90^\circ$, the critical time is zero, and the exponent is 1/2 for all times. In contrast, for $\theta < 90^\circ$, the exponent is 2/3, and it asymptotically approaches to 1/2. Recently, Ahmadlouydarab *et al.*[3] performed simulations to investigate coalescence of droplets on a wettability gradient surface. However, the asymmetric coalescence resulting due to coalescence of two unequal-sized droplets and coalescence of two droplets having different contact angles[26] due to a step gradient in wettability is still not well understood. In particular, it is not clear whether the scaling law of coalescence of equal-sized droplets is valid for asymmetric coalescence. Furthermore, a generalized analytical model that can predict both symmetric and asymmetric coalescence is not available.

To this end, we present a generalized analytical model to describe the inertial early-stage coalescence of two droplets on a solid surface. The model can be used to analyze coalescence of two equal-sized droplets, coalescence of two unequal-sized droplets, and coalescence of two droplets having different contact angles with the surface due to a step gradient in wettability. We study the evolution of the liquid bridge with time during coalescence. We supplement our analytical model with lattice Boltzmann method (LBM) simulations.

II. MATHEMATICAL MODEL FOR DROPLET COALESCENCE

Here, we present a generalized analytical model to study the coalescence of two droplets on a solid surface. Schematic illustrating the two-dimensional coalescence of two droplets of the same liquid having different contact angles with the surface due to a step gradient in surface wettability is shown in Fig. 1. Here, R_1 and R_2 are radii of the first and second drop, respectively, and the corresponding contact angles are θ_1 and θ_2, respectively. At $t = 0$, two droplets are in contact with each other as shown by the dotted line in Fig. 1. Later, a tiny liquid bridge connects both the droplets at the point of contact. The pressure in the bridge is lower due to infinite curvature of liquid bridge and this results in fluid flow from droplets to the bridge. Consequently, bridge height h_0 grows with time t.

The capillary pressure p_{cap} that drives the motion of liquid toward the liquid bridge and causes its growth scales as

$$p_{cap} \sim \frac{\sigma}{w}, \tag{1}$$

where σ and w denotes the surface tension and the radius of curvature of the bridge, respectively. The radius of curvature of the bridge w can be written as

$$w = \frac{1}{2}\Big[\Big(R_1 \sin\theta_1 - [R_1^2 - (h_0 + R_1\cos\theta_1)^2]^{1/2}\Big) + \Big(R_2 \sin\theta_2 - [R_2^2 - (h_0 + R_2\cos\theta_2)^2]^{1/2}\Big)\Big], \tag{2}$$

where h_0 is the bridge height at any instant of time t. The capillary pressure p_{cap} is balanced by the dynamic pressure p_{in} of the fluid and is given by

$$p_{in} \sim \rho v^2, \tag{3}$$

where v is the velocity of the fluid flowing into the bridge and is given as $v = \mathrm{d}h_0/\mathrm{d}t$. Equating Eqs. (1) and (3),

$$\rho\left(\frac{\mathrm{d}h_0}{\mathrm{d}t}\right)^2 = D_0\frac{\sigma}{w}, \tag{4}$$

where D_0 is a proportionality constant. Substituting the expression for w from Eq. (2) in Eq. (4), we obtain an ODE for $h_0(t)$,

$$\frac{\rho R_1 \sin\theta_1}{2\sigma}\left[\left(1-\left[\frac{1}{\sin^2\theta_1}-\left(\frac{h_0}{R_1\sin\theta_1}+\frac{1}{\tan\theta_1}\right)^2\right]^{1/2}\right)+\frac{R_2\sin\theta_2}{R_1\sin\theta_1}\left(1-\left[\frac{1}{\sin^2\theta_2}-\left(\frac{h_0}{R_2\sin\theta_2}+\frac{1}{\tan\theta_2}\right)^2\right]^{1/2}\right)\right]\times\left(\frac{\mathrm{d}h_0}{\mathrm{d}t}\right)^2 = D_0. \tag{5}$$

To nondimensionalize the above equation, we introduce the following dimensionless bridge height h_0^* and time t^*:

$$h_0^* = \frac{h_0}{R_1\sin\theta_1}, \quad t^* = \frac{t}{(\rho R_1^3\sin^3\theta_1/\sigma)^{1/2}}. \tag{6}$$

The nondimensionalized Eq. (5) in terms of these dimensionless variables is given by

$$\frac{1}{2}\left[\left(1-\left[\frac{1}{\sin^2\theta_1}-\left(h_0^*+\frac{1}{\tan\theta_1}\right)^2\right]^{1/2}\right)+\frac{1}{\beta}\left(1-\left[\frac{1}{\sin^2\theta_2}-\left(\beta h_0^*+\frac{1}{\tan\theta_2}\right)^2\right]^{1/2}\right)\right]\left(\frac{\mathrm{d}h_0^*}{\mathrm{d}t^*}\right)^2 = D_0, \tag{7}$$

where $\beta = (R_1\sin\theta_1)/(R_2\sin\theta_2)$. Equation (7) describes the evolution of dimensionless bridge height h_0^* with dimensionless time t^*. The bridge height depends on the shape of the coalescing droplets. The above equation can be used to study the coalescence of two equal-sized droplets, coalescence of two unequal-sized droplets and coalescence of two droplets having different contact angles with the surface. We solve above equation using the fourth-order Runge-Kutta method. We compare the solution of an analytical model with our two-dimensional LBM simulations. First, we revisit the problem of coalescence of two equal-sized droplets having the same contact angle θ with the surface and study the effect of contact angle on the bridge height. We then analyze the asymmetric coalescence resulting due to coalescence of two unequal-sized droplets and coalescence of two droplets having different contact angles due to a step gradient in wettability.

III. LATTICE BOLTZMANN SIMULATIONS

We employed a pseudopotential lattice Boltzmann method (LBM) to simulate droplet coalescence process on a solid surface. The LBM has developed into a powerful technique to simulate multiphase flows. In this approach, we do not require to track the interface as it inherently captures the interface due to interparticle interaction force between the fluid particles. Besides, there is no need to specify the dynamic contact angle as a function of contact line velocity.[27] Instead, the static contact angle is employed via a parameter in the interaction force between the fluid and solid particle. As a result, dynamic contact angle evolves during simulations. These characteristics make the LBM appropriate to simulate droplet coalescence process. We outline the lattice Boltzmann modeling here.

A. Pseudopotential lattice Boltzmann method

The temporal evolution of particle distribution function with Bhatnagar-Gross-Krook (BGK)[28] collision operator is given as,

$$f_i(\mathbf{x}+\mathbf{e}_i\delta t, t+\delta t) - f_i(\mathbf{x},t) = \frac{-1}{\tau}\left[f_i(\mathbf{x},t) - f_i^{eq}(\mathbf{x},t)\right] + \triangle f_i(\mathbf{x},t), \tag{8}$$

where $f_i(\mathbf{x},t)$ is the particle distribution function in the ith direction with discrete particle velocity $\mathbf{e}_i$ at location $\mathbf{x}$ and time t, τ is the dimensionless relaxation time and f_i^{eq} is corresponding equilibrium distribution function which is given by Yu *et al.*,[29]

$$f_i^{eq} = \rho w_i\left[1+3\frac{(\mathbf{e}_i\cdot\mathbf{u})}{c^2}+\frac{9}{2}\frac{(\mathbf{e}_i\cdot\mathbf{u})^2}{c^4}-\frac{3}{2}\frac{\mathbf{u}^2}{c^2}\right], \tag{9}$$

where $c = \delta x/\delta t$ is the lattice speed, δx and δt are the lattice spacing and time step, respectively, and w_i is a weighting factor. We use two-dimensional lattice arrangement with nine velocities (D2Q9) as shown in Fig. 2. The weighting factor w_i and discrete particle velocities for D2Q9 model are given as

$$w_i = \begin{cases} 4/9, & i=0, \\ 1/9, & i=1,2,3,4, \\ 1/36, & i=5,6,7,8, \end{cases} \tag{10}$$

$$\mathbf{e}_i = \begin{cases} (0,0), & i=0, \\ (\pm1,0)c, (0,\pm1)c, & i=1,2,3,4, \\ (\pm1,\pm1)c, & i=5,6,7,8. \end{cases} \tag{11}$$

Equation (8) is solved in two steps:

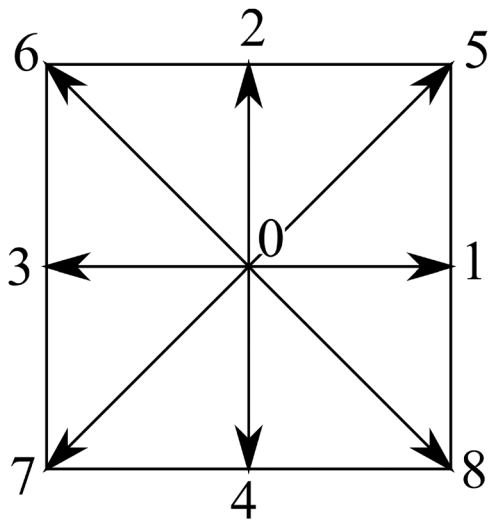

FIG. 2. Two-dimensional lattice arrangement with nine discrete velocities (D2Q9).

1. Collision:
   The particles arriving at a node collide and change their direction. The post collision distribution functions are calculated as

$$f_i^*(\mathbf{x},t) = f_i(\mathbf{x},t) - \frac{1}{\tau}\left[f_i(\mathbf{x},t) - f_i^{eq}(\mathbf{x},t)\right]. \tag{12}$$

2. Streaming:
   The particles move to the neighboring node corresponding to their velocity directions

$$f_i(\mathbf{x}+\mathbf{e}_i\delta t, t+\delta t) = f_i^*(\mathbf{x},t). \tag{13}$$

To implement the body force term $\Delta f_i(\mathbf{x},t)$, we used the exact difference method (EDM) proposed by Kupershtokh,[30,31]

$$\Delta f_i(\mathbf{x},t) = f_i^{eq}(\rho(\mathbf{x},t), \mathbf{u}+\Delta\mathbf{u}) - f_i^{eq}(\rho(\mathbf{x},t),\mathbf{u}), \tag{14}$$

where $\Delta\mathbf{u} = \mathbf{F}\delta t/\rho$ is velocity change due to the action of total force $\mathbf{F}$ during the time step Δt. The macroscopic density ρ and velocity $\mathbf{u}$ are calculated as

$$\rho = \sum_{i=0}^{b} f_i = \sum_{i=0}^{b} f_i^{eq}, \tag{15}$$

$$\rho\mathbf{u} = \sum_{i=0}^{b} f_i\mathbf{e}_i + \frac{\delta t}{2}\mathbf{F} = \sum_{i=0}^{b} f_i^{eq}\mathbf{e}_i + \frac{\delta t}{2}\mathbf{F}. \tag{16}$$

The kinematic viscosity ν is calculated using relaxation time τ by

$$\nu = c_s^2\left(\tau - \frac{1}{2}\right)\delta t, \tag{17}$$

where c_s is the speed of sound and given as $c_s = c/\sqrt{3}$.

The fluid particles (or pseudoparticles) resides on every lattice site. These particles interact via interaction forces. Therefore, we consider two types of interaction forces between the fluid and fluid particles, and between the fluid and the solid particles (or solid wall). Shan and Chen[32,33] introduced pesudopotential ψ to simulate nonlocal interactions between the fluid particles. For single-component multiphase flow, the interaction force acting on the particles at site $\mathbf{x}$ is given by[34]

$$\mathbf{F}_{\text{int}}(\mathbf{x}) = -\beta\psi(\mathbf{x})\sum_{\mathbf{x}'} G(\mathbf{x},\mathbf{x}')\psi(\mathbf{x}')(\mathbf{x}'-\mathbf{x}) - \frac{(1-\beta)}{2}\sum_{\mathbf{x}'} G(\mathbf{x},\mathbf{x}')\psi^2(\mathbf{x}')(\mathbf{x}'-\mathbf{x}), \tag{18}$$

where β is a constant factor and depends on the equation of state. For Peng-Robinson (P-R) equation of state, $\beta = 1.16$. The Greens function $G(\mathbf{x},\mathbf{x}')$ is given by

$$G(\mathbf{x},\mathbf{x}') = \begin{cases} g_1, & |\mathbf{x}'-\mathbf{x}| = 1, \\ g_2, & |\mathbf{x}'-\mathbf{x}| = \sqrt{2}, \\ 0, & \text{otherwise}, \end{cases} \tag{19}$$

where $g_1 = 2g$ and $g_2 = g/2$. The pseudopotential function ψ is given as[35]

$$\psi(\mathbf{x}) = \sqrt{\frac{2(p-\rho c_s^2)}{g c_s^2}}, \tag{20}$$

where p is the pressure and we used $g = -1$ in this study. The pressure p is calculated using Peng-Robinson (P-R) equation of state as given by[35]

$$p = \frac{\rho RT}{1-b\rho} - \frac{a\rho^2\varepsilon(T)}{1+2b\rho-b^2\rho^2}, \tag{21}$$

$$\varepsilon(T) = \left[1 + (0.37464 + 1.54226\omega - 0.26992\omega^2)\left(1 - \sqrt{\frac{T}{T_c}}\right)\right]^2,$$

where $a = 0.5472R^2T_c^2/p_c$ and $b = 0.0778RT/p_c$. In this work, we used $R = 1$, $a = 2/49$, $b = 2/21$. In addition, the interaction force between the fluid and the solid wall is given as[36]

$$\mathbf{F}_{\text{ads}}(\mathbf{x}) = -\left(1 - \exp^{-\rho(\mathbf{x})}\right)\sum_i G_{\text{ads}} w_i s(\mathbf{x}+\mathbf{e}_i\delta t)\cdot\mathbf{e}_i\delta t. \tag{22}$$

The parameter G_{ads} controls the strength of the interaction force between the fluid and the solid wall. The different contact angles are obtained by adjusting G_{ads} values, and $s(\mathbf{x}+\mathbf{e}_i\delta t)$ is an indicator function which is expressed as

$$s(\mathbf{x}+\mathbf{x}\delta t) = \begin{cases} 0 & \text{if } (\mathbf{x}+\mathbf{e}_i\delta t) \text{ is fluid node}, \\ 1 & \text{if } (\mathbf{x}+\mathbf{e}_i\delta t) \text{ is solid node}. \end{cases}$$

Therefore, the total force acting at each site $\mathbf{x}$ is given by

$$\mathbf{F} = \mathbf{F}_{\text{int}} + \mathbf{F}_{\text{ads}}. \tag{23}$$

IV. RESULTS AND DISCUSSION

In this section, we present results obtained from a mathematical model and LBM simulations. We have shown a detailed validation of code in our previous paper.[6] We considered three cases: (i) coalescence of equal-sized droplets on a surface with homogeneous wettability, (ii) coalescence of unequal-sized droplets on a surface with homogeneous wettability, and (iii) coalescence of droplets having different contact angles with the surface due to a step gradient in wettability. For all simulations, we used following fluid properties: $\rho_l = 692.37$ kg/m^3, $\rho_v = 53.85$ kg/m^3, $\nu_l = 1.19 \times 10^{-7}$ m^2/s, and $\nu_v = 3.74 \times 10^{-7}$ m^2/s. Conversion of physical units to lattice units can be found in our previous paper.[6]

Figure 3 shows the schematic of the computation domain for equal-sized droplets. We performed two-dimensional simulations in

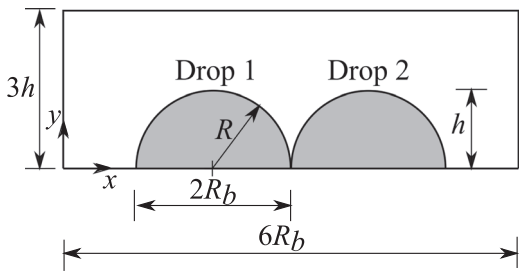

FIG. 3. Schematic of the computational domain for coalescence of two equal-sized droplets on a surface with homogeneous wettability. We defined solid walls at the bottom and the upper boundary and employed the bounce-back scheme. The periodic condition was specified in the x-direction. Initially, two droplets of identical radius R were placed on the bottom wall.

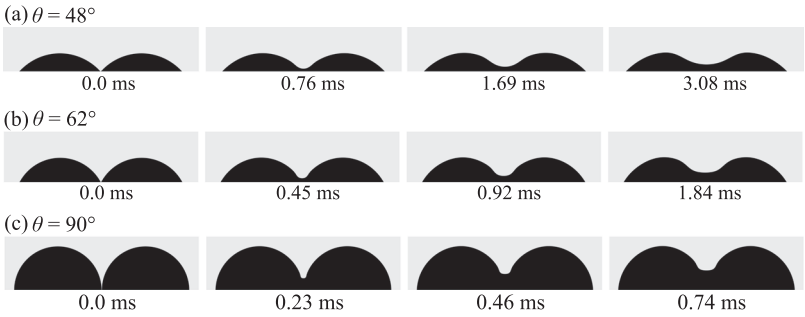

FIG. 4. Contours of droplet coalescence on homogeneous surfaces with different contact angles at different times in the early-stage coalescence. The bridge height grows faster on a substrate with larger contact angle.

a rectangular domain of $6R_b \times 3h$ lattice units, where R_b and h are the base radius and the height of a droplet, respectively. We defined solid walls at the bottom and the upper boundary, and employed the bounce-back scheme. Periodic boundary condition was specified in the x-direction. Initially, two droplets of identical radius R were placed on the bottom wall. The droplets were separated by a distance of 4 lattice units. The initial separation of the droplets has no influence on the results. The droplets were separated by a distance of 4 lattice units. We also varied the initial separation distance for a few cases, and we observed that the initial separation distance does not influence the simulation predictions. This ensures that the growth dynamics is independent of the initial condition. Therefore, we have performed all simulations with the same initial condition, i.e., droplets are separated by a distance of 4 lattice units.

The thickness of the interface is around 4–5 lattice units in our simulations. We ensured that the bridge height h_0 is significantly larger than the interface thickness. Also, the scaling laws are valid in the very early stage of the coalescence. Therefore, in this work the bridge height h_0 ranges from $0.1h$ to $0.4h$.[20] The position of the liquid-vapor interface corresponds to a density value of $\rho_{\text{interface}} = (\rho_l + \rho_v)/2$.

We also performed grid independent study to check the effect of grid size on simulation results. We considered two droplets of 150 μm radius each on a substrate with the contact angle of 90°. We performed simulations with three grid resolutions of droplet sizes, namely, 500, 750, and 1000 lattice units, while keeping the same Ohnesorge number Oh. Here, we define the Ohnesorge number $Oh = \mu/\sqrt{\rho\sigma R_b}$ as the ratio of viscous to inertia and surface tension forces. We have calculated the Ohnesorge number Oh based on base radius R_b of droplet 1. We find no significant difference between the droplet size 750 and 1000 lattice units. Therefore, for all simulations reported in this work, we used droplet size of 750 lattice units which corresponds to $\Delta x = 0.2$ μm and $\Delta t = 4.63 \times 10^{-2}$ μs.

A. Coalescence of two equal-sized droplets on homogeneous surfaces

First, we study the effect of surface wettability on the coalescence process. We performed simulations on surfaces with homogeneous wettability having contact angles of 48°, 62°, 77°, and 90°. For all simulations, we fixed the total volume of droplet as 7.06×10^{-3} mm^3. The values of the Ohnesorge number values are 0.0371, 0.0393, 0.0418, and 0.0441 for simulation cases with contact angles 48°, 62°, 77°, and 90°, respectively. Figure 4 shows contours of droplet coalescence on surfaces with uniform contact angle of 48°, 62°, and 90°. The bridge height h_0 grows with time t and at long times magnitude of bridge height is of the order of droplet size.

For the coalescence of two equal-sized droplets, Eq. (7) simplifies to the equation derived by the Sui *et al.*,[25] i.e.,

$$\left(1 - \left[\frac{1}{\sin^2\theta} - \left(h_0^* + \frac{1}{\tan\theta}\right)^2\right]^{1/2}\right)\left(\frac{dh_0^*}{dt^*}\right)^2 = D_0. \quad (24)$$

Figure 5 shows the comparison of the mathematical model Eq. (24) and the LBM simulations for coalescence of equal-sized droplets. However, the proportionality constant D_0 varies with the contact angle θ of the surface. We used values of D_0 as 0.22, 0.4, 0.66, and 1.0 for contact angles of 48°, 62°, 77°, and 90°, respectively to match with LBM simulations. The simulation results are in agreement with the mathematical model. We observe that bridge height h_0^* grows faster on a substrate with a larger contact angle. This is explained as follows: For the same volume of liquid, the droplet radius decreases with the increase of contact angle θ and, as a result, the curvature

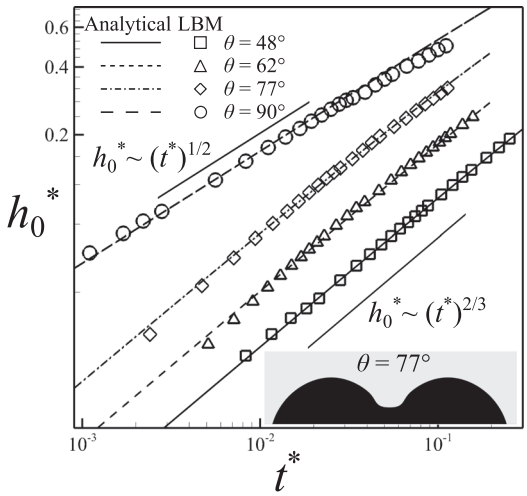

FIG. 5. Coalescence of equal-sized droplets on a surface with homogeneous wettability. Evolution of bridge height with time for different contact angles. We rescaled bridge height h_0 with the base radius R_b and time t with inertial time scale $\sqrt{\rho R_b^3/\sigma}$. Data points show the bridge height predicted by LBM simulations. Lines show the bridge height predicted by the analytical model.

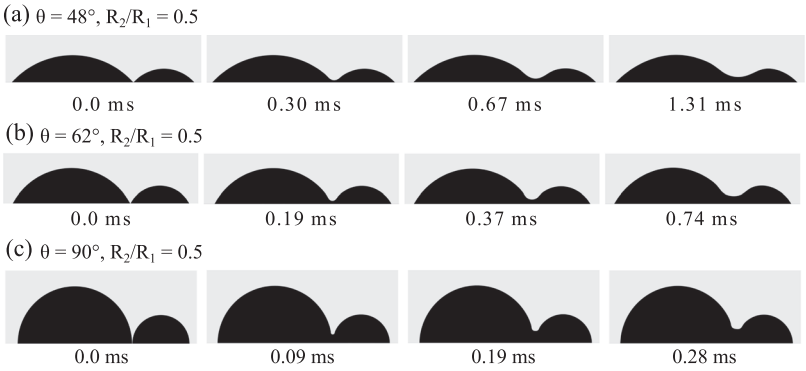

FIG. 6. Contours of coalescence of two unequal-sized droplets on a surface with homogeneous wettability. We fixed the radius of droplet 1 and varied the radius of droplet 2 such that $R_2/R_1 = 0.5$.

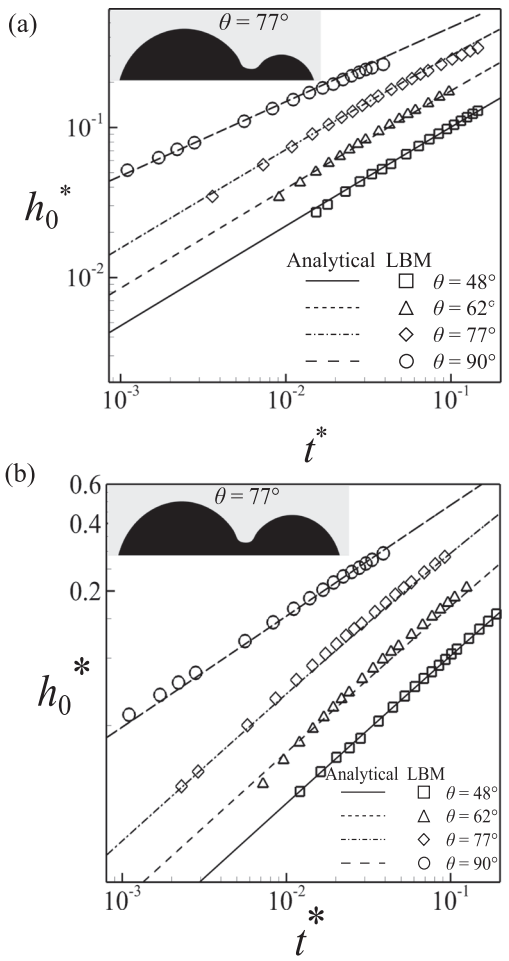

FIG. 7. Comparison of bridge height predicted by mathematical model and LBM simulations for coalescence of two unequal-sized droplets on a surface with homogeneous wettability. Data points and lines show the bridge height predicted by LBM simulations and mathematical model, respectively. (a) $R_2/R_1 = 0.5$. (b) $R_2/R_1 = 0.75$. The bridge height scales with time as $h_0^* \sim (t^*)^{2/3}$ for $\theta < 90°$ and $h_0^* \sim (t^*)^{1/2}$ for $\theta = 90°$.

($\sim 1/R$) of droplet increases with θ. Moreover, the radius of curvature w of the bridge also decreases with an increase in θ, and, therefore, pressure in liquid bridge p_{bridge} decrease. This results in higher capillary pressure on the surface with a higher contact angle and, subsequently, more amount of liquid flows toward the bridge. Therefore, bridge height increases at faster rate on a surface with larger contact angle. We also observe that the dimensionless bridge height h_0^* follows the power law $h_0^* \sim (t^*)^{1/2}$ for $\theta = 90°$ and $h_0^* \sim (t^*)^{2/3}$ for $\theta < 90°$. This disparity in power law exponent can be explained as below. Taylor series expansion of the first term $(1 - [1/\sin\theta - (h_0^* + 1/\tan\theta)^2]^{1/2})$ of Eq. (24) for a variable h_0^* around $h_0^* = 0$ up to second order terms of h_0^* gives

$$\left[\frac{h_0^*}{\tan\theta} + \frac{(h_0^*)^2}{2}\left(1 + \frac{1}{\tan^2\theta}\right)\right]\left(\frac{dh_0^*}{dt^*}\right)^2 = D_0. \tag{25}$$

For $\theta = 90°$, the above equation gives $h_0^* \sim (t^*)^{1/2}$. On the other hand, for $\theta < 90°$, the first term $(h_0^*/\tan\theta)$ dominates because $h_0^* \ll 1$. Therefore, bridge height scales with time as $h_0^* \sim (t^*)^{2/3}$.

B. Coalescence of two unequal-sized droplets on homogeneous surfaces

In this section, we discuss the coalescence of two unequal-sized droplets (or asymmetric coalescence) on surfaces with homogeneous wettability. For simulations presented here, we fixed the radius of droplet 1 and varied the radii of droplet 2 such that $R_2/R_1 = 0.5$, 0.75, and 1.0. For all simulations, we fixed the total volume of droplet 1 as 7.06×10^{-3} mm^3.

TABLE I. The values of proportionality constant D_0 for different contact angles used in Eq. (26).

	Proportionality constant D_0	
Contact angle θ (deg)	$R_2/R_1 = 0.5$	$R_2/R_1 = 0.75$
48	0.18	0.20
62	0.33	0.34
77	0.55	0.57
90	0.67	0.78

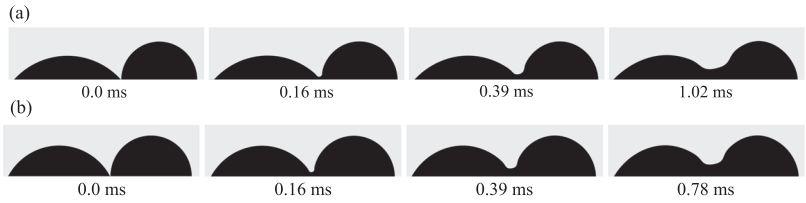

FIG. 8. Contours of coalescence of two droplets of same liquid having different contact angles with the surface due to a step gradient in wettability. (a) The contact angles of droplets 1 and 2 are 62° and 90°, respectively. (b) The contact angles of droplets 1 and 2 are 77° and 90°, respectively.

Figure 6 shows the time-lapse images of the bridge profile for $R_2/R_1 = 0.5$ for surfaces with uniform contact angles of 48°, 62°, and 90°. The coalescence process of unequal-sized droplets differs from that of equal-sized droplets due to asymmetric droplet meniscus shape. After initial contact, due to capillary pressure, liquid from both sides flows into the liquid bridge. However, the capillary pressure difference $\Delta p_1 < \Delta p_2$, where Δp_1 and Δp_2 are the capillary pressure difference between the large droplet and the liquid bridge, and small droplet and the liquid bridge, respectively. Therefore, more amounts of liquid flows toward the bridge from the smaller droplet compared to the larger droplet. Finally, the smaller droplet is absorbed into the larger droplet. For the coalescence of two unequal-sized droplets on a surface with uniform contact angle, Eq. (7) simplifies to

$$\frac{1}{2}\left[\left(1-\left[\frac{1}{\sin^2\theta}-\left(h_0^*+\frac{1}{\tan\theta}\right)^2\right]^{1/2}\right)+\frac{R_2}{R_1}\times\left(1-\left[\frac{1}{\sin^2\theta}-\left(\frac{R_1}{R_2}h_0^*+\frac{1}{\tan\theta}\right)^2\right]^{1/2}\right)\right]\left(\frac{dh_0^*}{dt^*}\right)^2=D_0. \quad (26)$$

Figures 7(a) and 7(b) shows the comparison of mathematical model Eq. (26) and LBM simulations for $R_2/R_1 = 0.5$ and $R_2/R_1 = 0.75$, respectively. The values of proportionality constant D_0 for different contact angles are listed in Table I. The simulation results are in agreement with the mathematical model. We observe that the same scaling law of coalescence of equal-sized droplets is valid for coalescence of unequal-sized droplets and explained as below. Taylor series expansion of the first term $0.5[(1-[1/\sin^2\theta-(h_0^*+1/\tan\theta)^2]^{1/2})+R_2/R_1(1-[1/\sin^2\theta-(R_1/R_2\,h_0^*+1/\tan\theta)^2]^{1/2})]$ of Eq. (26) for a variable h_0^* around $h_0^*=0$ up to second order terms of h_0^* gives

$$\left[\frac{h_0^*}{\tan\theta}+\frac{(h_0^*)^2}{2}\left(1+\frac{1}{\tan^2\theta}\right)\frac{R_1+R_2}{2R_2}\right]\left(\frac{dh_0^*}{dt^*}\right)^2=D_0. \quad (27)$$

For $\theta = 90°$, the above equation gives $h_0^* \sim (t^*)^{1/2}$. In contrast, for $\theta < 90°$, the first term $(h_0^*/\tan\theta)$ dominates because $h_0^* \ll 1$. Therefore, the bridge height scales with time as $h_0^* \sim (t^*)^{2/3}$.

C. Coalescence of two droplets of same liquid having different contact angles with the surface due to a step gradient in wettability

In this section, we analyze the coalescence of two droplets of the same liquid having different contact angles with the surface due to a step gradient in wettability. The surface $x < 3R_b$ has $\theta = 90°$ and for $x \geq 3R_b$ has $\theta < 90°$. First, we fixed the contact angle of droplet 2 as $\theta_2 = 90°$ and varied the contact angle of droplet 1 such that $\theta_1 < 90°$. We set the total volume as 7.06×10^{-3} mm^3 for both droplets having different contact angles with the surface. Figure 8 shows the contours of coalescence of two droplets of same liquid with contact angles of droplet 1 and droplet 2 are 62° and 90°, respectively. In this case also, due to different contact angles of droplets with the surface, the shape of the meniscus is asymmetric.

Figure 9 shows the comparison of mathematical model and LBM simulations for $\theta_1 < 90°$ and $\theta_2 = 90°$. We used values of D_0 as 0.45, 0.60, 0.68, and 0.80 for contact angles of 48°–90°, 62°–90°, 69°–90°, and 77°–90°, respectively, to match with LBM simulations. The simulation results matches with the mathematical model. We observe that for all cases, bridge height h_0^* grows as $h_0^* \sim (t^*)^{2/3}$. Although, the contact angle of the second droplet is 90°, bridge height grows with $(t^*)^{2/3}$. To understand the reason behind the scaling law $(t^*)^{2/3}$ irrespective of the contact angle θ, we performed the Taylor series expansion of Eq. (7). Taylor series expansion of first term $0.5[(1-[1/\sin^2\theta-(h_0^*+1/\tan\theta_1)^2]^{1/2})+1/\beta(1-[1/\sin^2\theta-(\beta h_0^*+1/\tan\theta_2)^2]^{1/2})]$ of Eq. (7) for a variable h_0^* around $h_0^*=0$ up to the second order terms of h_0^* gives

$$\left(\frac{h_0^*}{2}\left(\frac{1}{\tan\theta_1}+\frac{1}{\tan\theta_2}\right)+\frac{(h_0^*)^2}{4}\times\left[\left(1+\frac{1}{\tan^2\theta_1}\right)+\beta\left(1+\frac{1}{\tan^2\theta_2}\right)\right]\right)\left(\frac{dh_0^*}{dt_0^*}\right)^2=D_0. \quad (28)$$

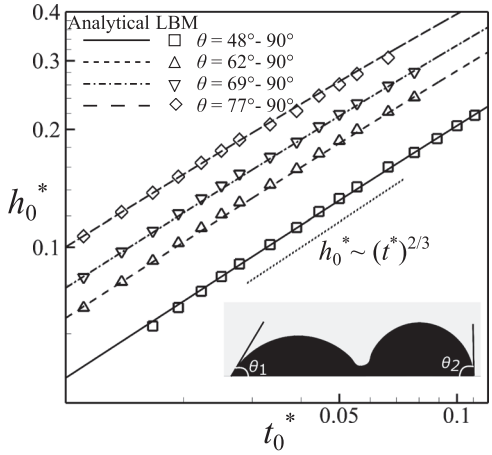

FIG. 9. Comparison of bridge height predicted by the mathematical model and LBM simulations for coalescence of two droplets of same liquid having different contact angles with the surface due to a step gradient in wettability. Data points and lines show the bridge height predicted by LBM simulations and mathematical model, respectively. The surface $x < 3R_b$ has $\theta = 90°$ and for $x \geq 3R_b$ has $\theta < 90°$.

For $\theta_1 < 90^\circ$ and $\theta_2 = 90^\circ$, the first term $h_0^*/2(1/\tan\theta_1)$ dominates because $h_0^* \ll 1$. However, this term is a function of θ_1 only. Therefore, bridge growth depends on the lower contact angle of droplet θ_1 and we get the power law $h_0^* \sim (h_0^*)^{2/3}$. Similarly, for both $\theta_1 < 90^\circ$ and $\theta_2 < 90^\circ$, we can easily show that the nondimensional bridge height grows with dimensionless time as $h_0^* \sim (h_0^*)^{2/3}$.

V. CONCLUSIONS

We have investigated symmetric and asymmetric coalescence of two droplets on a solid surface. For low viscosity liquids, such as water, inertia dominates viscous effects, and hence, coalescence occurs in the inertia-dominated regime. We have proposed a generalized analytical model to study the coalescence of two droplets. The model can be used to predict the growth of a liquid bridge for coalescence of two equal-sized droplets, coalescence of two unequal-sized droplets, and coalescence of two droplets having different contact angles with the surface due to a step gradient in wettability. We also supplemented results of the mathematical model with LBM simulations based on the pseudopotential multiphase model. The results showed that for the coalescence of two equal-sized droplets on a surface with homogeneous wettability, the growth of a liquid bridge scales with time as $(t^*)^{1/2}$ and $(t^*)^{2/3}$ for $\theta = 90^\circ$ and $\theta < 90^\circ$, respectively. We also demonstrated that the same scaling relation is valid for the coalescence of two unequal-sized droplets on a surface with homogeneous wettability. In addition to coalescence of equal and unequal-sized droplets, we have discussed the coalescence of two droplets of the same liquid having different contact angles with the surface due to a step gradient in wettability. We showed that irrespective of contact angles, the bridge height scales with time as $h_0^* \sim (t^*)^{2/3}$.

ACKNOWLEDGMENTS

The authors gratefully acknowledge the financial support from the Department of Science and Technology (DST), India via the INSPIRE fellowship (Award No. IFA12-ENG-15). The authors also thank IIT Delhi HPC facility for computational resources.

APPENDIX: RADIUS OF CURVATURE *w* OF THE LIQUID BRIDGE

Here, we provide the detailed derivation of Eq. (2) for the radius of curvature w of the liquid bridge. Figure 10 shows the geometry of the coalescence of two liquid droplets of the same liquid having different contact angles with the surface due to a step gradient in surface wettability.

The radius of curvature of the bridge w is partly in the region having contact angle θ_1 and partly in the region having contact angle θ_2. Therefore, we take the radius of curvature of the bridge w as the average of w_1 and w_2 as given below,

$$w = \frac{1}{2}(w_1 + w_2). \tag{A1}$$

From $\triangle OAB$, we can obtain the distance OB as given by

$$x_1 = \left[R_1^2 - (h_0 + R_1\cos\theta_1)^2\right]^{1/2}. \tag{A2}$$

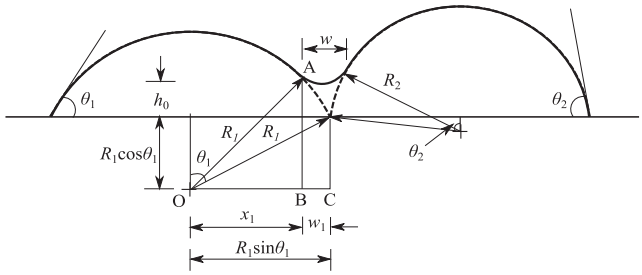

FIG. 10. Schematic of the coalescence of two droplets of same liquid having different contact angles with the surface.

Since $x_1 + w_1 = R_1 \sin\theta_1$, we obtain w_1 as given below,

$$w_1 = R_1\sin\theta_1 - \left[R_1^2 - (h_0 + R_1\cos\theta_1)^2\right]^{1/2}. \tag{A3}$$

Similarly, we can also obtain w_2 as given by

$$w_2 = R_2\sin\theta_2 - \left[R_2^2 - (h_0 + R_2\cos\theta_2)^2\right]^{1/2}. \tag{A4}$$

From Eq. (A1), we get

$$w = \frac{1}{2}\Big[(R_1\sin\theta_1 - \left[R_1^2 - (h_0 + R_1\cos\theta_1)^2\right]^{1/2}) + (R_2\sin\theta_2 - \left[R_2^2 - (h_0 + R_2\cos\theta_2)^2\right]^{1/2})\Big]. \tag{A5}$$

REFERENCES

[1]J. D. Paulsen, R. Carmigniani, A. Kannan, J. C. Burton, and S. R. Nagel, "Coalescence of bubbles and drops in an outer fluid," Nat. Commun. **5**, 3182 (2014).
[2]M. Wu, T. Cubaud, and C.-M. Ho, "Scaling law in liquid drop coalescence driven by surface tension," Phys. Fluids **16**, L51–L54 (2004).
[3]M. Ahmadlouydarab, C. Lan, A. K. Das, and Y. Ma, "Coalescence of sessile microdroplets subject to a wettability gradient on a solid surface," Phys. Rev. E **94**, 033112 (2016).
[4]R. C. Srivastava, "Size distribution of raindrops generated by their breakup and coalescence," J. Atmos. Sci. **28**, 410–415 (1971).
[5]W. W. Grabowski and L.-P. Wang, "Growth of cloud droplets in a turbulent environment," Annu. Rev. Fluid Mech. **45**, 293–324 (2013).
[6]N. D. Pawar, S. R. Kale, S. S. Bahga, H. Farhat, and S. Kondaraju, "Study of microdroplet growth on homogeneous and patterned surfaces using lattice Boltzmann modelling," J. Heat Transfer **141**, 062406 (2019).
[7]M. Singh, N. D. Pawar, S. Kondaraju, and S. S. Bahga, "Modeling and simulation of dropwise condensation: A review," J. Indian Inst. Sci. **99**, 157–171 (2019).
[8]B. Derby, "Inkjet printing of functional and structural materials: Fluid property requirements, feature stability, and resolution," Annu. Rev. Mater. Res. **40**, 395–414 (2010).
[9]L. Duchemin, J. Eggers, and C. Josserand, "Inviscid coalescence of drops," J. Fluid Mech. **487**, 167–178 (2003).
[10]R. W. Hopper, "Coalescence of two equal cylinders: Exact results for creeping viscous plane flow driven by capillarity," J. Am. Ceram. Soc. **67**, C–262 (1984).
[11]R. W. Hopper, "Stokes flow of a cylinder and half-space driven by capillarity," J. Fluid Mech. **243**, 171–181 (1992).
[12]R. W. Hopper, "Coalescence of two viscous cylinders by capillarity: Part I, theory," J. Am. Ceram. Soc. **76**, 2947–2952 (1993).
[13]D. G. A. L. Aarts, H. N. W. Lekkerkerker, H. Guo, G. H. Wegdam, and D. Bonn, "Hydrodynamics of droplet coalescence," Phys. Rev. Lett. **95**, 164503 (2005).
[14]S. C. Case and S. R. Nagel, "Coalescence in low-viscosity liquids," Phys. Rev. Lett. **100**, 084503 (2008).

[15]J. Eggers, J. R. Lister, and H. A. Stone, "Coalescence of liquid drops," J. Fluid Mech. **401**, 293–310 (1999).
[16]J. F. Hernández-Sánchez, L. A. Lubbers, A. Eddi, and J. H. Snoeijer, "Symmetric and asymmetric coalescence of drops on a substrate," Phys. Rev. Lett. **109**, 184502 (2012).
[17]S. Mitra and S. K. Mitra, "Symmetric drop coalescence on an under-liquid substrate," Phys. Rev. E **92**, 033013 (2015).
[18]W. D. Ristenpart, P. M. McCalla, R. V. Roy, and H. A. Stone, "Coalescence of spreading droplets on a wettable substrate," Phys. Rev. Lett. **97**, 064501 (2006).
[19]R. D. Narhe, D. A. Beysens, and Y. Pomeau, "Dynamic drying in the early-stage coalescence of droplets sitting on a plate," Europhys. Lett. **81**, 46002 (2008).
[20]M. W. Lee, D. K. Kang, S. S. Yoon, and A. L. Yarin, "Coalescence of two drops on partially wettable substrates," Langmuir **28**, 3791–3798 (2012).
[21]S. S. Thete, "Singularities in free surface flows," Ph.D. thesis, Purdue University, 2016.
[22]J. D. Paulsen, J. C. Burton, S. R. Nagel, S. Appathurai, M. T. Harris, and O. A. Basaran, "The inexorable resistance of inertia determines the initial regime of drop coalescence," Proc. Natl. Acad. Sci. U. S. A. **109**, 6857–6861 (2012).
[23]J. D. Paulsen, "Approach and coalescence of liquid drops in air," Phys. Rev. E **88**, 063010 (2013).
[24]A. Eddi, K. G. Winkels, and J. H. Snoeijer, "Influence of droplet geometry on the coalescence of low viscosity drops," Phys. Rev. Lett. **111**, 144502 (2013).
[25]Y. Sui, M. Maglio, P. D. M. Spelt, D. Legendre, and H. Ding, "Inertial coalescence of droplets on a partially wetting substrate," Phys. Fluids **25**, 101701 (2013).
[26]M. Singh, S. Kondaraju, and S. S. Bahga, "Mathematical model for dropwise condensation on a surface with wettability gradient," J. Heat Transfer **140**, 071502 (2018).
[27]I. Roisman, L. Opfer, C. Tropea, M. Raessi, J. Mostaghimi, and S. Chandra, "Drop impact onto a dry surface: Role of the dynamic contact angle," Colloids Surf., A **322**, 183–191 (2008).
[28]P. L. Bhatnagar, E. P. Gross, and M. Krook, "A model for collision processes in gases. I. small amplitude processes in charged and neutral one-component systems," Phys. Rev. **94**, 511–525 (1954).
[29]D. Yu, R. Mei, L.-S. Luo, and W. Shyy, "Viscous flow computations with the method of lattice Boltzmann equation," Prog. Aerosp. Sci. **39**, 329–367 (2003).
[30]A. Kupershtokh and D. Medvedev, "Lattice Boltzmann equation method in electrohydrodynamic problems," J. Electrost. **64**, 581–585 (2006).
[31]A. Kupershtokh, D. Medvedev, and D. Karpov, "On equations of state in a lattice Boltzmann method," Comput. Math. Appl. **58**, 965–974 (2009), mesoscopic methods in engineering and science.
[32]X. Shan and H. Chen, "Lattice Boltzmann model for simulating flows with multiple phases and components," Phys. Rev. E **47**, 1815–1819 (1993).
[33]X. Shan and H. Chen, "Simulation of nonideal gases and liquid-gas phase transitions by the lattice Boltzmann equation," Phys. Rev. E **49**, 2941–2948 (1994).
[34]S. Gong and P. Cheng, "A lattice Boltzmann method for simulation of liquid-Vapor phase-change heat transfer," Int. J. Heat Mass Transfer **55**, 4923–4927 (2012).
[35]P. Yuan and L. Schaefer, "Equations of state in a lattice Boltzmann model," Phys. Fluids **18**, 042101 (2006).
[36]M. C. Sukope and D. T. Thorne, *Lattice Boltzmann Modeling: An Introduction for Geoscientists and Engineers* (Springer-Verlag, Berlin Heidelberg, 2006).